Improved method for studying the propagation dynamics of ultrafast electron pulses based on mean-field models*

Meng-Chao Li(李梦超)[1,2], Xuan Wang(王瑄)[1,†], Guo-Qian Liao(廖国前)[1], Yu-Tong Li(李玉同)[1,2,3,‡], and Jie Zhang(张杰)[3,4]

[1] *Beijing National Laboratory for Condensed Matter Physics, Institute of Physics, Chinese Academy of Sciences, Beijing* 100190, *China*
[2] *School of Physical Sciences, University of Chinese Academy of Sciences, Beijing* 100049, *China*
[3] *Collaborative Innovation Centre of Inertial Fusion Science and Applications, Shanghai Jiao Tong University, Shanghai* 200240, *China*
[4] *Department of Physics, Shanghai Jiao Tong University, Shanghai* 200240, *China*

(Received 18 December 2016; revised manuscript received 22 February 2017; published online 6 April 2017)

We have studied the propagation dynamics of ultrafast electron pulses by using an improved mean-field model, in which the propagation of the electron pulses across the boundary of the acceleration region is explicitly considered. A large decrease in the speed spread of the electron pulses (we called "boundary kick") is observed and properly treated leading to a significant improvement in the simulation accuracy, particularly when the density of electrons is very large. We show that our method is consistent with the simulation by the *N*-particle method, while others can introduce factorial error.

Keywords: ultrafast electron diffraction, space-charge, mean-field, charge particle propagation

PACS: 41.85.Ja, 61.05.Jd, 29.27.Bd, 06.60.Jn **DOI:** 10.1088/1674-1056/26/5/054103

1. Introduction

Ultrafast electron diffraction (UED) technique gets a rapid development recently in various research areas, which holds great promise for resolving ultrafast processes with atomic level details.[1–8] One of the key issues in UED is how to obtain ultrashort bright electron pulses, whose longitudinal pulse width dominates the overall temporal resolution. However, the repulsive force among electrons (or space-charge effect) tends to broaden the pulse during its propagation, which limits the number of electrons per pulse for different applications and also affects the overall performance of UED systems. Therefore, a deep understanding of the propagation dynamics of ultrashort electron pulses, particularly the evolution of its longitudinal width due to space-charge effect is critical. Although this topic has been extensively discussed in other research areas such as accelerator physics,[9,10] the available tools are not straightly applicable and usually overkill for typical UED parameter space. Qian first introduced a one-dimensional "fluid model" to give analytical solutions for the longitudinal pulse broadening for UED.[11] Then a more general mean-field model has been developed by various groups.[12–16] The simulation results explain the observation very well.[17,18] Meanwhile, *N*-particle numerical methods have also been developed which give more accurate prediction[10,19,20] but are computationally intensive. Nevertheless, mean-field models can provide an intuitive physical picture which the *N*-particle method is usually lacking.

A typical UED set up studied previously is shown in Fig. 1(b), which is also the prototype of several UED apparatus.[2–5,21] The electrons (blue) are emitted from the cathode by laser excitation and then are accelerated by a static electric field to reach very high energy (typically 10 keV to 100 keV). To avoid the distortion of acceleration field around the pin hole of the anode, which can de-focus the beam transversely, a metal mesh is attached on it.[2,3,11,15] After leaving the anode, electrons will freely drift to the sample and be diffracted. Other components such as deflection coil, magnetic lens, beam compressor, and so on can be added to further collimate the electron beam during its propagation,[14,19] but the effect of these components on the electron propagation is not considered in this article. In previous analytical studies, the whole propagation process is separated into acceleration and free drift regions (Region 1 and 3 in Fig. 1(b)). On the other hand, how electrons cross the boundary between these two regions is not discussed. Figure 1(d) highlights such a process in the boundary region (Region 2). In this region, some electrons are freely drifting while the others are still accelerating. As a result, the velocity difference between the electrons in the front and the tail (or velocity spread of the electron pulse) will decrease. Such an effect, which is called "boundary kick", can be clearly seen in the *N*-particle simulation,[10] however, it is not accounted explicitly by the mean-field method. In this article, we carefully studied the propagation dynamics of electron pulses in all three regions, particularly in the boundary region. We found that the effect of the boundary became extremely important when the electron density was large. Under such

*Project supported by the National Basic Research Program of China (Grant No. 2013CBA01501) and the Science Challenge Program and the Strategic Pilot Project of the Chinese Academy of Sciences.

†Corresponding author. E-mail: xw@iphy.ac.cn
‡Corresponding author. E-mail: ytli@iphy.ac.cn

© 2017 Chinese Physical Society and IOP Publishing Ltd

condition, the simulation result of our improved mean-field model was consistant with the N-particle simulation result, while the one without considering the boundary region introduced factorial error. The validity of previous mean-field models for the electron propagation dynamics is also discussed.

2. Analytical model

We study the propagation dynamics of ultra-short electron pulses based on mean-field models, the details of which have been explained elsewhere.[11,12,14,15] Briefly, an electron pulse is treated as a smooth charge density profile (see Fig. 1(a)). The mutual interactions between each individual electron are treated approximately by using a homogenous field (mean field), resulting from this charge density profile. Driven by this mean field, the pulse will expand both longitudinally and transversely. The whole process is separated in three regions following Fig. 1:

$$l(t)=\begin{cases} l_1(t), & t_0\le t\le t_{\rm I},\\ l_2(t), & t_{\rm I}\le t\le t_{\rm II},\\ l_3(t), & t_{\rm II}\le t,\end{cases}$$
$$r(t)=\begin{cases} r_1(t), & t_0\le t\le t_{\rm I},\\ r_2(t), & t_{\rm I}\le t\le t_{\rm II},\\ r_3(t), & t_{\rm II}\le t,\end{cases} \quad (1)$$

where $l(t)$ and $r(t)$ represent the longitudinal and transverse lengths of an electron pulse measured between the half maximum points (FWHM) of a smooth charge density distribution (for example, Gaussian function), or between the edge points of a distribution that cuts off sharply (for example, top-hat function) in the lab frame (LF). However, such definition sometimes brings ambiguity when comparing $l(t)$ and $r(t)$ for different density distribution profiles. Hence the dimensions that cover the same amount of electrons are usually used, for example, 76% of $l(t)$ for a top-hat function is used when compared with the FWHM for a Gaussian function. In the right hand side of Eqs. (1), a subscript number is added to $l(t)$ or $r(t)$ to indicate the three different regions. We also define the longitudinal velocity spread as

$$v(t)=\frac{{\rm d}l(t)}{{\rm d}t}. \quad (2)$$

When working in the center-of-momentum inertial frame (CFM), a prime is added to these notations. For example, $l'(t')$ represents the transformation of $l(t)$ into CFM. Another fundamental assumption for mean-field models is that a velocity chirp must be built up longitudinally and transversely such that the closer electrons to the center, the slower they are moving against it.

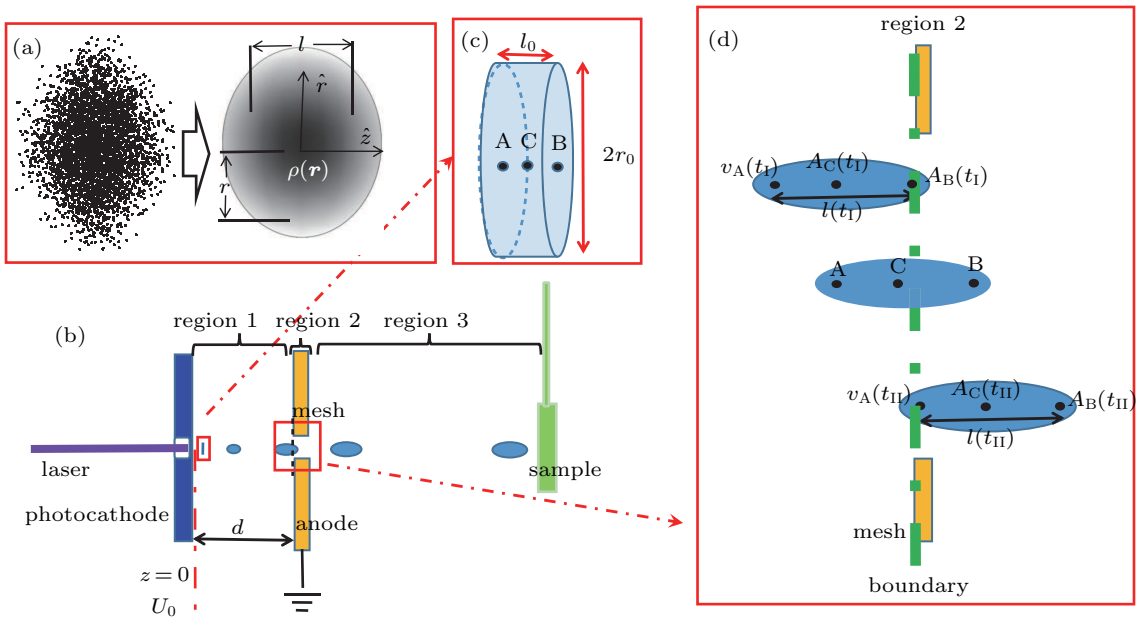


Fig. 1. (color online) (a) Conceptual sketch for the mean-field approach. A bunch of discrete electrons is treated as a smooth charge density profile. (b) A schematic diagram of an ultrafast electron diffraction system. The trajectory of electrons is separated into three regions. (c) An enlarged plot of a cylindrically symmetric electron bunch (in this case with a top-hat charge density distribution). A, B and C are the tail, front and center of the bunch. (d) A highlight of the boundary region.

Our method separates the electron propagation into three regions.

2.1. Region 1: acceleration

This region accounts for the propagation of electron pulses from the cathode ($z=0$) within the acceleration electric field E_z until the front of it (point B) reaches the edge of the anode ($z=d$). Although the center–of–momentum of the electron pulse (point C) is accelerating, an inertial frame that moves at the same speed of C can be chosen for each time instance. The dynamical equations of electron pulses in such

CMF can be written as

$$\begin{cases} \dfrac{\mathrm{d}^2 l_1'(t')}{\mathrm{d}t'^2} = K\dfrac{1}{\kappa^{\mathrm{L}}} f_{\mathrm{MF-L}}, \\ \dfrac{\mathrm{d}^2 r_1'(t')}{\mathrm{d}t'^2} = K\dfrac{1}{\kappa^{\mathrm{T}}} f_{\mathrm{MF-T}}, \\ K = \dfrac{Ne^2}{m_{\mathrm{e}}\varepsilon_0 \pi r_1'^2}, \end{cases} \tag{3}$$

where $f_{\mathrm{MF-L}}$ and $f_{\mathrm{MF-R}}$ are the mean-field functions depending on $l_1'(t')$ and $r_1'(t')$ with κ^{L} and κ^{T} as the correction factor respectively depending on the density distribution function.[15] K is a constant with N, m_{e}, e, and ε_0 as the number electrons per pulse, the mass of an electron, the charge of an electron, and the permittivity of the vacuum respectively. Also, the effects of collimation components such as magnetic lens, pulse compressor, and so on, are not included in Eqs. (3), since they are not the focus of this article. During the formation of the electron pulse by laser excitation, the speed of C is still very small and therefore the relativistic effect can be simply ignored and all the quantities in CMF are equal to their values in LF. Then, the initial conditions to solve Eqs. (3) can be written as

$$\begin{cases} \left.\dfrac{\mathrm{d}l_1'(t')}{\mathrm{d}t'}\right|_{t'=t_0'} = v_{\mathrm{L}}, \\ \left.\dfrac{\mathrm{d}r_1'(t')}{\mathrm{d}t'}\right|_{t'=t_0'} = v_{\mathrm{R}}, \\ l_1'(t_0') = l(t_0'), \\ r_1'(t_0') = r(t_0'), \end{cases} \tag{4}$$

where $l(t_0')$ and $r(t_0')$ are the initial longitudinal pulse length and radius respectively. v_{R} and v_{L} are the initial speed spread in the two directions respectively. If we assume that the initial photoelectrons have a Gaussian energy distribution with an energy spread of ΔE as FWHM, and a random special distribution in the illumination area of the cathode, then v_{R} can be estimated by

$$v_{\mathrm{R}} = 2\sqrt{\frac{2\Delta E}{m_{\mathrm{e}}}}. \tag{5}$$

However, the N-particle method indicates that v_{R} calculated in this way is slightly bigger than the real velocity spread. This is because it takes time for electrons to redistribute (without space charge effect) to fulfill the velocity chirp condition for the mean-field methods. On the other hand, v_{L} contains contributions from both ΔE and the acceleration by the extraction field E_z', which equals E_z under the reference frame transformation. To get an upper limit of v_{L}, we simply add these two contributions together

$$v_{\mathrm{L}} = \sqrt{\frac{2\Delta E}{m_{\mathrm{e}}}} + \frac{eE_z}{m_{\mathrm{e}}}\tau_{\mathrm{laser}}, \tag{6}$$

where τ_{laser} is the laser pulse length. Since the second term in Eq. (6) provides the velocity chirp, v_{L} is close to the real value proved by N-particle simulation. Nevertheless, v_{R} and v_{L} are only important for a very small number of electrons per pulse where the space charge is not so significant. Accordingly, $l(t_0')$ can be written as

$$l(t_0') = \sqrt{\frac{2\Delta E}{m_{\mathrm{e}}}}\tau_{\mathrm{laser}} + \frac{eE_{\mathrm{z}}}{2m_{\mathrm{e}}}\tau_{\mathrm{laser}}^2. \tag{7}$$

Equation set (3) are numerically solved until t_{I}', when the front of the pulse (point B) reaches the boundary (in the LF)

$$z_{\mathrm{B1}}(t_{\mathrm{I}}') = z_{\mathrm{C1}}(t_{\mathrm{I}}') + \frac{l_1(t_{\mathrm{I}}')}{2\gamma_{\mathrm{C1}}(t_{\mathrm{I}}')} = d. \tag{8}$$

$z_{\mathrm{C1}}(t')$ is the position of C that can be written as[22]

$$z_{\mathrm{C1}}(t') = \frac{m_{\mathrm{e}}c^2}{eE_z}\left(\cosh\left(\frac{eE_z t'}{m_{\mathrm{e}}c}\right) - 1\right) + \frac{l(t_0')}{2}. \tag{9}$$

$\gamma_{\mathrm{C1}}(t')$ is the relativistic factor which could be calculated by[22]

$$\gamma_{\mathrm{C1}}(t') = \cosh\left(\frac{eE_z t'}{m_{\mathrm{e}}c}\right). \tag{10}$$

By solving Eqs. (8)–(10), t_{I}' evaluated and is converted to t by[22]

$$t(t') = \frac{m_{\mathrm{e}}c}{eE_z}\sinh\left(\frac{eE_z t'}{m_{\mathrm{e}}}\right). \tag{11}$$

2.2. Region 2: boundary region

In this region, the front of the electron pulse has entered the drift region while the tail of the pulse still accelerates for a short time interval of $t_{\mathrm{I}} - t_{\mathrm{II}}$. So the kinematics of A and B must be considered separately by

$$\begin{cases} \dfrac{\mathrm{d}^2 z_{\mathrm{B2}}'(t')}{\mathrm{d}t'^2} = K\dfrac{1}{2\kappa^{\mathrm{L}}} f_{\mathrm{MF-L}}, \\ \dfrac{\mathrm{d}^2 z_{\mathrm{A2}}'(t')}{\mathrm{d}t'^2} = -K\dfrac{1}{2\kappa^{\mathrm{L}}} f_{\mathrm{MF-L}} + \dfrac{eE_z'}{m_{\mathrm{e}}}, \end{cases} \tag{12}$$

where $z_{\mathrm{B2}}'(t')$ and $z_{\mathrm{A2}}'(t')$ are the positions of B and A in the CMF in Region 2 respectively. Then $l_2'(t')$ can be written as

$$\frac{\mathrm{d}^2 l_2'(t')}{\mathrm{d}t'^2} = \frac{\mathrm{d}^2 z_{\mathrm{B2}}'(t')}{\mathrm{d}t'^2} - \frac{\mathrm{d}^2 z_{\mathrm{A2}}'(t')}{\mathrm{d}t'^2} = K\frac{1}{\kappa^{\mathrm{L}}} f_{\mathrm{MF-L}} - \frac{eE_z'}{m_{\mathrm{e}}}. \tag{13}$$

Comparing with Eqs. (3), it can be seen that the dynamics of the electron pulse in the boundary region is very different. Meanwhile, the equation for the transverse direction is the same as in Region 1

$$\frac{\mathrm{d}^2 r_2'(t')}{\mathrm{d}t'^2} = K\frac{1}{\kappa^{\mathrm{T}}} f_{\mathrm{MF-T}}. \tag{14}$$

The initial conditions for this region are

$$\begin{cases} \left.\dfrac{\mathrm{d}l_2'(t')}{\mathrm{d}t'}\right|_{t'=t_{\mathrm{I}}'} = \left.\dfrac{\mathrm{d}l_1'(t')}{\mathrm{d}t'}\right|_{t'=t_{\mathrm{I}}'}, \\ \left.\dfrac{\mathrm{d}r_2'(t')}{\mathrm{d}t'}\right|_{t'=t_{\mathrm{I}}'} = \left.\dfrac{\mathrm{d}r_1'(t')}{\mathrm{d}t'}\right|_{t'=t_{\mathrm{I}}'}, \\ l_2'(t_{\mathrm{I}}') = l_1'(t_{\mathrm{I}}'), \\ r_2'(t_{\mathrm{I}}') = r_1'(t_{\mathrm{I}}'). \end{cases} \tag{15}$$

Since the acceleration by the mean field (first term in Eq. (13)) is much smaller than the external field (second term), it is ignored during the calculation. Then from Eq. (13) we get

$$v'\left(t'\right)=\frac{\mathrm{d}l_2'\left(t'\right)}{\mathrm{d}t'}=\left.\frac{\mathrm{d}l_1'\left(t'\right)}{\mathrm{d}t'}\right|_{t'=t_{\mathrm{I}}'}-\frac{eE_{\mathrm{z}}'}{m_{\mathrm{e}}}\left(t'-t_{\mathrm{I}}'\right), \tag{16}$$

According to Eq. (16), $v'\left(t'\right)$ is reduced at the boundary, which we called "boundary kick". Simulation by using Eq. (13) is finished until t_{II}, when A leaves the boundary

$$z_{\mathrm{A2}}\left(t_{\mathrm{II}}\right)=d. \tag{17}$$

Since the space charge effect can be ignored if comparing with the effect from E_z', the kinetics of A in LF can be written as

$$\begin{cases}\dfrac{\mathrm{d}^2z_{\mathrm{A2}}\left(t\right)}{\mathrm{d}t^2}=\dfrac{eE_z}{\gamma_{\mathrm{C1}}\left(t_{\mathrm{I}}\right)m_{\mathrm{e}}},\\ \left.\dfrac{\mathrm{d}z_{\mathrm{A2}}\left(t\right)}{\mathrm{d}t}\right|_{t=t_{\mathrm{I}}}=\left.\dfrac{\mathrm{d}z_{\mathrm{A1}}\left(t\right)}{\mathrm{d}t}\right|_{t=t_{\mathrm{I}}},\\ z_{\mathrm{A2}}\left(t_{\mathrm{I}}\right)=d-l\left(t_{\mathrm{I}}\right),\end{cases} \tag{18}$$

where $\left.\dfrac{\mathrm{d}z_{\mathrm{A1}}\left(t\right)}{\mathrm{d}t}\right|_{t=t_{\mathrm{I}}}$ can be evaluated by the velocity transformation from CMF to LF

$$\frac{\mathrm{d}z_{\mathrm{A1}}\left(t_{\mathrm{I}}\right)}{\mathrm{d}t}=\frac{v_{\mathrm{A1}}'\left(t_{\mathrm{I}}'\right)+v_{\mathrm{C1}}\left(t_{\mathrm{I}}'\right)}{1+\dfrac{v_{\mathrm{A1}}'\left(t_{\mathrm{I}}'\right)v_{\mathrm{C1}}\left(t_{\mathrm{I}}'\right)}{c^2}}, \tag{19}$$

with

$$v_{\mathrm{A1}}'\left(t_{\mathrm{I}}'\right)=-\frac{1}{2}\left.\frac{\mathrm{d}l_1'\left(t'\right)}{\mathrm{d}t'}\right|_{t'=t_{\mathrm{I}}'}, \tag{20}$$

and v_{C1} is the velocity of the center-of-momentum in the LF. Ignoring the change of $\gamma_{\mathrm{C1}}\left(t\right)$ in the short time interval of $t_{\mathrm{II}}-t_{\mathrm{I}}$, equation (13) can be solved by using t_{II} and $v_{\mathrm{A}}\left(t_{\mathrm{II}}\right)$ determined by Eq. (16) through Eq. (20).

2.3. Region 3: free drift

In this region, the dynamical equations for electron pulses are the same as Region 1

$$\begin{cases}\dfrac{\mathrm{d}^2l_3'\left(t'\right)}{\mathrm{d}t'^2}=K\dfrac{1}{\kappa^{\mathrm{L}}}f_{\mathrm{MF-L}},\\ \dfrac{\mathrm{d}^2r_3'\left(t'\right)}{\mathrm{d}t'^2}=K\dfrac{1}{\kappa^{\mathrm{T}}}f_{\mathrm{MF-T}},\end{cases} \tag{21}$$

with the initial conditions

$$\begin{cases}\left.\dfrac{\mathrm{d}l_3'\left(t'\right)}{\mathrm{d}t'}\right|_{t'=t_{\mathrm{II}}'}=\left.\dfrac{\mathrm{d}l_2'\left(t'\right)}{\mathrm{d}t'}\right|_{t'=t_{\mathrm{II}}'},\\ \left.\dfrac{\mathrm{d}r_3'\left(t'\right)}{\mathrm{d}t'}\right|_{t'=t_{\mathrm{II}}'}=\left.\dfrac{\mathrm{d}r_2'\left(t'\right)}{\mathrm{d}t'}\right|_{t'=t_{\mathrm{II}}'},\\ l_3'\left(t_{\mathrm{II}}'\right)=l_2'\left(t_{\mathrm{II}}'\right),\\ r_3'\left(t_{\mathrm{II}}'\right)=r_2'\left(t_{\mathrm{II}}'\right).\end{cases} \tag{22}$$

Table 1. Simulation parameters.

	N-particle method		Mean-field	
	Longitudinal	Transverse	Longitudinal	Transverse
Length/m	$l\left(t_0'\right)=19\times10^{-9}$	$r\left(t_0'\right)=66.7\times10^{-6}$	$l\left(t_0'\right)=19\times10^{-9}$	$r\left(t_0'\right)=66.7\times10^{-6}$
Density distribution	Gaussian profile	Gaussian profile	Gaussian profile	Gaussian profile
velocity spread/m·s^{-1}	NA	NA	$v_{\mathrm{L}}=4.32\times10^5$	$v_{\mathrm{R}}=4.58\times10^5$
Velocity distribution	Gaussian profile (FWHM: 0.3 eV)[23]	Gaussian profile (FWHM: 0.3 eV)[23]	NA	NA
Mean-field function.[14]	NA	NA	$f_{\mathrm{MF-L}}=1-\dfrac{l}{\sqrt{l^2+4r^2}}$, $\kappa^{\mathrm{L}}=2$	$f_{\mathrm{MF-T}}=\dfrac{1}{\pi}$, $\kappa^{\mathrm{T}}=2$
Laser duration/fs	50	NA	50	NA

3. Simulation result

To demonstrate the significance of our improved mean-field model, we studied the propagation dynamics of the UED set-up as shown in Fig. 1. The acceleration voltage is set to be $U_0=100$ kV between cathode and anode, which are separated by $d=8$ mm. The intensity profile of the pumping laser is assumed to be a Gaussian function with its FWHM of 50 femtoseconds (fs). As a comparison, the N-particle method is also used. As mentioned before, to more accurately determine v_{R}, we first used the N-particle method without space-charge to linearly fit v_{R} in order to account for the formation of velocity chirp transversely, which can improve the accuracy of about 5% for very few electrons per pulse ($N=10^4$). Other parameters used in the simulation are summarized in Table 1.

Figures 2 and 4 show the dimensions and the spread velocity of an electron pulse as a function of time for three different numbers of electrons per pulse simulated by mean-field models and the N-particle method. It can be seen that our method is consistent with the result of the N-particle method. The difference between the two methods is within ten percent for electron numbers below one million. As the number of electrons further increases, the difference between the two tends to enlarge. This is because the density distribution function in the pulse also evolves due to the space charge effect,[14] which is not accounted by the mean-field models.

To demonstrate the significance of the "boundary kick", the electron propagation dynamics in the longitudinal direction around Region 2 is highlighted in each figure. It can be

seen that the spread velocity of the pulse $v(t)$ drastically decreased when passing the boundary. Such "boundary kick" can be separated into a model-related trivial part and a space-charge-related non-trivial part. Assuming that electrons have no charges (no space charge effect), the energy gained by each electron is the same in the acceleration region. Then the velocity spread after passing the boundary can be calculated by

$$\begin{cases} m_e c^2 + eU = \gamma_A(t_{II}) m_e c^2, \\ m_e c^2 + eU + \Delta E = \gamma_B(t_{II}) m_e c^2, \end{cases} \tag{23}$$

which yields an essentially small $v_2(t_{II})$

$$\begin{aligned} v_2(t_{II}) &= v_B(t_{II}) - v_A(t_{II}) \approx \frac{\Delta E}{\gamma_C^3(t_{II}) m_e v_C(t_{II})} \\ &\approx v_L \frac{v_L}{2\gamma_C^3(t_{II}) v_C(t_{II})}. \end{aligned} \tag{24}$$

These two equations should also be valid in our model under no space-charge condition. Since the aforementioned process is separately analyzed in Region 1 and Region 2, and the acceleration within τ_{laser} has been accounted by v_L (see the second term in Eq. (6)), $v_1(t)$ must sharply decrease to be nearly zero in Region 2 in this case, then the magnitude of "boundary kick" can be estimated by

$$\begin{aligned} \Delta v_{kick} &\approx v_{ns}(t_I) - v_L \frac{v_L}{2\gamma_C^3(t_{II}) v_C(t_{II})} \\ &\approx v_{ns}(t_I), \end{aligned} \tag{25}$$

where $v_{ns}(t_I)$ represents the velocity spread of the electron pulse at the boundary under no space-charge condition. We called this part the model-related trivial part of "boundary kick", because, as we will show later, this effect can be included in previous mean-field models without even considering Region 2 but only for a small number of electrons per pulse.

Moreover, if the space-charge effect is turned on, it causes a significant increase of longitudinal pulse length together with velocity spread in Region 1. Therefore, equation (24) does not hold any longer. Since electrons at the tail retreat relative to those in front, not only does the velocity spread increase, but they are accelerated for a longer time before leaving Region 1, which gives the extra space-charge related non-trivial "boundary kick".[19] The relative significance of these two parts depends on the number density of electrons per pulse n_e. When n_e is small, the trivial part dominates and $v_1(t)$ decreases to almost zero in Region 2 as shown in Fig. 2(c) (see the black diamond curve). Also, $v_1(t)$ is dominated by v_L in Region 1. On the other hand, when n_e is large, the non-trivial part dominates as shown in Fig. 4(c). In this case, an initial increase of $v_1(t)$ due to the space-charge effect is observed which is not so obvious in Fig. 2(c), followed by a decrease due to the relativistic effect, the same as in Fig. 2(c). Both $v_1(t_I)$ and $v_2(t_{II})$ are dominated by the space-charge effect, which is much larger than v_L.

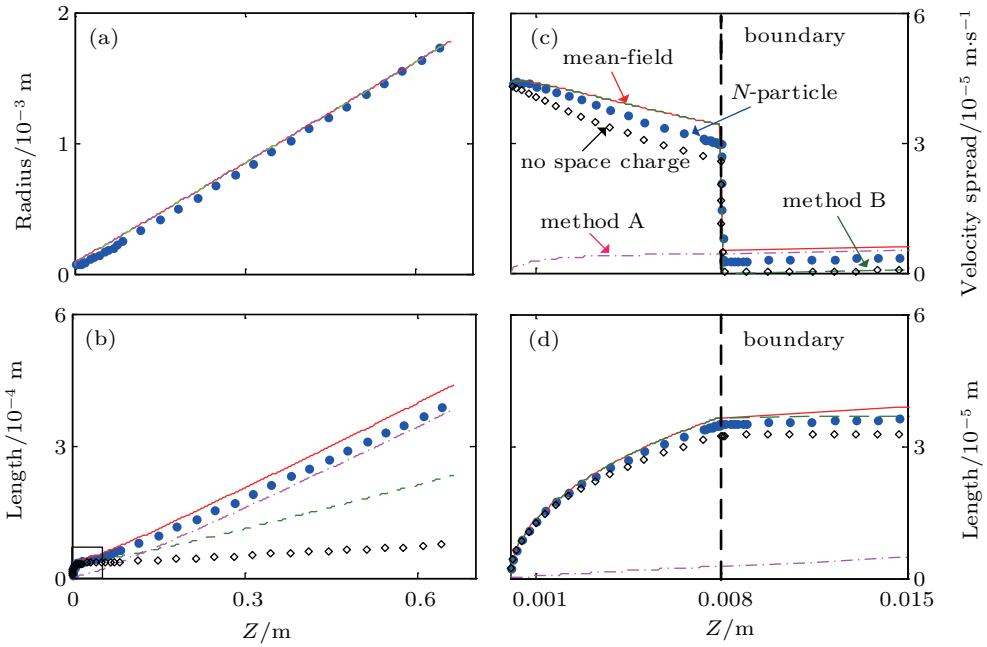


Fig. 2. (color online) Temporal evolution of pulse radius (a) and pulse length (b) for 10^4 electron per pulse simulated by the N-particle method (blue dotted) and our improved mean-field model (red solid). (c) and (d) are the enlarged view of the pulse length and the corresponding velocity spread as a function of time for the area marked in the black square in (b), which highlights Region 1 and Region 2. As a comparison, simulations by two other methods (see context for details) that ignore the boundary region are also shown (pink dash-dot line for method A and green dashed line for method B). An N-particle simulation for electrons with no space-charge effect is also presented (black diamond), and the sharp change of velocity spread at the boundary shows the trivial part of "boundary kick".

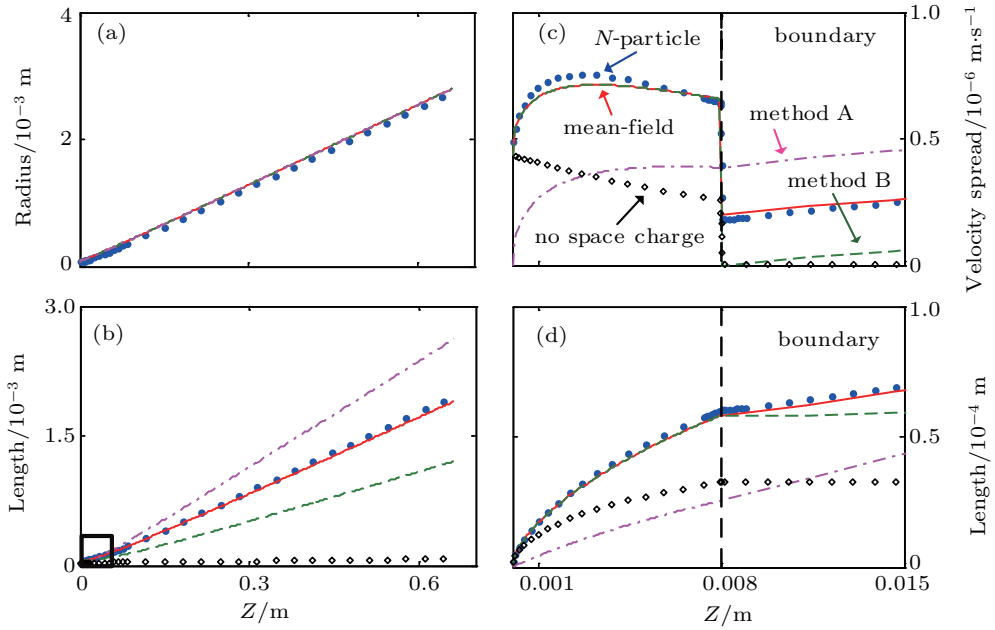


Fig. 3. (color online) Temporal evolution of pulse radius (a) and pulse length (b) for 10^5 electron per pulse simulated by the *N*-particle method (blue dotted) and our improved mean-field model (red solid). (c) and (d) are the enlarged view of the pulse length and the corresponding velocity spread as a function of time for the area marked in the black square in (b), which highlights Region 1 and Region 2. As a comparison, simulations by the other two methods (see context for details) that ignore the boundary region are also shown (pink dash-dot line for method A and green dashed line for method B). An *N*-particle simulation for electrons with no space-charge effect is also presented (black diamond), and the sharp change of velocity spread at the boundary shows the trivial part of "boundary kick".

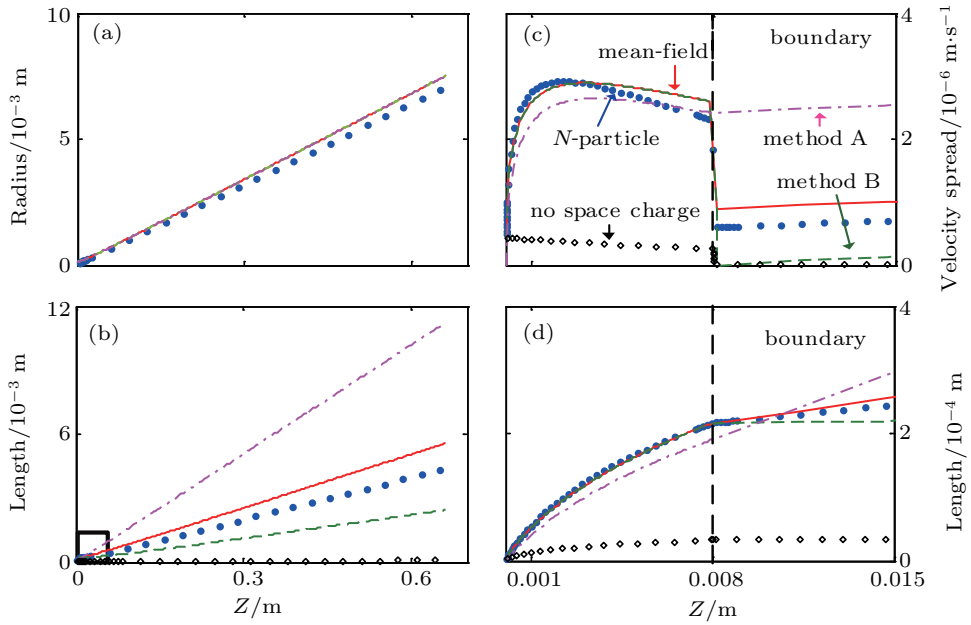


Fig. 4. (color online) Temporal evolution of pulse radius (a) and pulse length (b) for 10^6 electron per pulse simulated by the *N*-particle method (blue dotted) and our improved mean field model (red solid). (c) and (d) are the enlarged view of the pulse length and the corresponding velocity spread as a function of time for the area marked in the black square in panel (b), which highlights Region1 and Region 2. As a comparison, simulations by two other methods (see context for details) that ignore the boundary region are also shown (pink dash-dot line for method A and green dashed line for method B). An *N*-particle simulation for electrons with no space-charge effect is also presented (black diamond), and the sharp change of velocity spread at the boundary shows the trivial part of "boundary kick".

In previous studies, Region 1 and 2 are either ignored because the total time in these two regions is much smaller than in Region 3, or they are treated the same as in Region 3 (we define as method A) by using Eq. (21) and Eq. (22). In the former case, certain approximation of the initial conditions for Eq. (21) must be used. For example, it is usually assumed that the pulse length is determined by the laser pulse width, and the initial velocity spread is negligible. As shown in our analysis, such an assumption is only valid when the trivial "boundary kick" dominates and therefore limits the application of these

models for small n_e. The same principle also applies for the latter case, where the initial velocity spread in Eq. (22) must be set to zero. Even with these considerations, these methods usually underestimate the longitudinal pulse width at the early time of propagation (see the comparison of method A with N-particle simulation from Fig. 2(d) to Fig. 4(d)). On the other hand, Qian (we define as method B) developed a model that separately considered Region 1 and Region 3 by the same principle as our model, although Qian used a mean-field formula only suitable for $l \ll r$ (or 1D fluid model). The big difference between Qian's model and ours lies in Region 2. Since Qian's model assumes that $l(t)$ is dominated by initial velocity spread in Region 1 and space-charge effect in Region 3 respectively, it simply adds these two components together (see the last paragraph of Page 6 in Ref. [11]). Such treatment is only valid for small n_e, where the space-charge effect is negligible in Region 1. It is also equivalent to set $v_2(t_{II})$ to be zero for Region 3 and again only valid when the trivial "boundary kick" dominates. As a comparison, the simulation results by Qian's model are also plotted in Figs. 2–4. Here, we replace his mean-field formula by those used in this article such that the space-charge effect is not ignored in Region 1 and is more accurately calculated through the whole process. It can be seen that even for $N = 10^4$, the space-charge effect in Region 1 cannot be neglected and it becomes more and more important as the number of electrons increases. Qian's model gives about 30% to 40% errors for all cases. As a comparison, our improved method gives much better results.

4. Conclusion

We use an improved method based on mean-field models to study the propagation dynamics of electron pulses in which the boundary effect of the acceleration region is explicitly considered. A big decrease of velocity spread at the boundary is observed and properly treated. The simulation result is consistent with the N-particle method. The origin of the boundary effect is further separated into the model-related trivial part and space-charge related non-trivial part. Particularly, the non-trivial part has not been considered by previous studies and therefore can introduce factorial error in the simulation when the number density of electrons per pulse is large.

Acknowlegdements

The authors would like to thank Xiao-Ju Li from the College of Material Science and Engineering of Changchun University of Technology for our helpful discussion.

References

[1] Mourou G and Williamson S 1982 *Appl. Phys. Lett.* **41** 44
[2] Cao J, Hao Z, Park H, Tao C, Kau D and Blaszczyk L 2003 *Appl. Phys. Lett.* **83** 1044
[3] Siwick B J, Dwyer J R, Jordan R E and Miller R J 2003 *Science* **302** 1382
[4] Ihee H, Lobastov V A, Gomez U M, Goodson B M, Srinivasan R, Ruan C Y and Zewail A H 2001 *Science* **291** 458
[5] Ruan C Y, Vigliotti F, Lobastov V A, Chen S and Zewail A H 2004 *Proc. Natl. Acad. Sci.* **101** 1123
[6] Centurion M, Reckenthaeler P, Trushin S A, Krausz F and Fill E E 2008 *Nat. Photon.* **2** 315
[7] King W E, Campbell G H, Frank A and Reed B 2005 *J. Appl. Phys.* **97** 111101
[8] Liang W X, Zhu P F, Wang X, Nie S H, Zhang Z C, Cao J M, Sheng Z M and Zhang J 2009 *Acta. Phys. Sin.* **58** 5546 (in Chinese)
[9] Reiser M 2008 *Theory and Design of Charged Particle Beams* (2nd edn) (New York: Wiley)
[10] van der Geer S B, de Loos M J, Oudheusden T V, op.'t. Root W P E M, van. der. Wiel M J and Luiten O J 2006 *Phys. Rev. Spec. Top-AC* **9** 192
[11] Qian B L and Elsayed-Ali H E 2002 *J. Appl. Phys.* **91** 462
[12] Siwick B J, Dwyer J R, Jordan R E and Miller R J D 2002 *J. Appl. Phys.* **92** 1643
[13] Qian B L and Elsayed-Ali H E 2003 *J. Appl. Phys.* **94** 803
[14] Collin S, Merano M, Gatri M, Sonderegger S, Renucci P, Ganiére J D and Deveaud B 2005 *J. Appl. Phys.* **98** 094910
[15] Reed B W 2006 *J. Appl. Phys.* **100** 034916
[16] Michalik A M and Sipe J E 2006 *J. Appl. Phys.* **99** 054908
[17] Wang X, Nie S, Park H, Li J, Clinite R, Li R, Wang X and Cao J 2009 *Rev. Sci. Instrum.* **80** 013902
[18] Gahlmann A, Tae P S and Zewail A H 2008 *Phys. Chem. Chem. Phys.* **10** 2894
[19] Oudheusden T V 2010 *Electron Source for sub-relativistic Single-shot Femtosecond Diffraction* (Ph. D. Thesis) (Netherlands Eindhoven: Eindhoven University of Technology)
[20] Van O T, Pasmans P L, Sb V D G, de Loos M J, Mj V D W and Luiten O J 2010 *Phys. Rev. Lett.* **105** 172
[21] Pei M J, Qi D L, Qi Y P, Jia T Q, Zhang S A and Sun Z R 2015 *Acta Phys. Sin.* **64** 165 (in Chinese)
[22] Misner C W, Thorne K S, Wheeler J A, Misner C W, Thorne K S and Wheeler J A 1997 *Gravitation* (Taiwan, China: CKS Bookstore) pp. 163–176
[23] Passlack S, Mathias S, Andreyev O, Mittnacht D, Aeschlimann M and Bauer M 2006 *J. Appl. Phys.* **100** 024912